Guided modes modeling in multilayered composites plates

Morched Ben Amor

Faculté des Sciences de Sfax, Laboratoire de Physique des Matériaux, BP 802, 3018 Sfax, Tunisia
morched_benamor@yahoo.fr

Due to the periodicity of the composite structure the Floquet wave approach seems well suited for multilayered medium characterization. The pass and stop band domains for [0/45/90/-45] cross ply composites have been plotted. Dispersive guided wave propagation through a lossy composite laminates immersed in water have been investigated. Our interest is focused on a guided mode inside the frequency range from 1.6 MHz to 5 MHz. Within the considered frequency range, these modes have been pointed out by both reflection coefficient and density of energy analysis in term of incident angle. In this paper it is investigated how by fine-tuning the frequency and the incident angle, internal displacement and stress field vary in the multilayer. When the frequency is increased the mode changes from a plate mode to a surface mode. The description includes real Floquet wave numbers as well as complex wave numbers.

1 Introduction

Multilayered systems are extensively used in many engineering areas (automotive and aeronautic fields among others). These materials are stacked of orthotropic laminas which assembled in different periodic stacking sequences of fibber directions to form multilayered structures as shown in Fig.1. Thus, such systems are highly anisotropic multilayered structures, which significantly complicate ultrasonic wave propagation [1,2,3]. The selection of ultrasonic inspection parameters is very difficult for these structures without comprehensive modelling for optimization of the experimental conditions and data interpretation.
In such structures, modal waves, which propagate with a phase velocity in the direction of the layers plane, can be brought to the fore: they can be analogous to Lamb waves when the structure is finite in depth or Rayleigh-type when the structure is a semi-infinite periodic medium. In the last case, several Rayleigh wave families do exist and are dispersive, like Lamb waves; these waves have been called ‘‘multilayered Rayleigh waves’’ [4,5].

Extensive studies of wave propagation in laminated composites were started in the 1960 by Achenbach and co-workers [6] considering the laminate layers as isotropic. They described spectra of guided and Floquet waves and discuss a low frequency homogenization using static effective moduli theory. Shull et al [7] showed that the special Lamb wave dispersion behaviour is caused by the pass and stop bands of the Floquet waves in a plate containing four layers of aluminium and three layers of aramid-epoxy composite lamina. There are few works on leaky waves that behaves as Rayleigh waves in infinite periodically stratified anisotropic media. In 1999, Potel et al studies the existence of multilayered Rayleigh modes in anisotropic periodically multilayered media.

The main objective of the paper is to study the guided wave in a lossy multilayered composite medium. In section 2, the stiffness matrix method for wave propagation in layered generally anisotropic media is briefly recalled. In section 3, the ultrasonic reflection and transmission characteristics are calculated according to the incident angles θ at different frequencies. Dispersive guided wave propagation through a loss composite laminates immersed in water have been investigated in section 4. The Floquet wave spectra in angle and frequency domains are used for interpretation of the results. In this paper it is investigated how by fine-tuning the frequency, the incident angle, internal displacement and stress profiles vary in the multilayer. The energy distribution inside the composite plate can also be used to detect the guided mode.

2 Backgrounds

2.1 Stiffness matrix

In this section we will elucidate the stiffness matrix solution for generally anisotropic layers in a form suitable for multilayered system analysis. Let us consider a multilayered plate, consisting of *N* arbitrarily viscoelastic anisotropic layers as illustrated in Fig. 1.

In the jth layer, the displacement vector u_j may be written as the summation of six partial waves [8]:

$$u_j = \sum_{\eta=1}^{3} (a_\eta^d P_\eta^d e^{ik_z^d (z - z_{j-1})} + a_\eta^u P_\eta^u e^{ik_z^u (z - z_j)})_j \, e^{i(k_x x + k_y y - \omega t)} \quad (1)$$

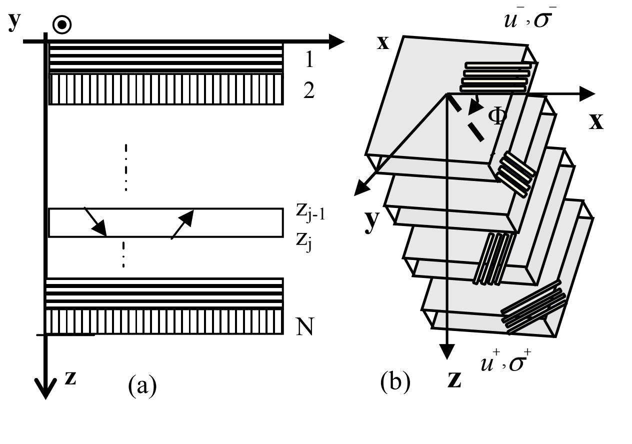

Fig.1 (a) Periodic structure (b) Unit cell, coordinate system

Where $u_j = (u_x, u_y, u_z)_j^T$, $\eta = (1,2,3)$ denotes ηth partial wave and T represents the transpose. The superscripts d and u represent the downward (+z) and the upward (-z) travelling plane wave modes respectively; $P_\eta^{d,u} = (P_x^{d,u}, P_y^{d,u}, P_z^{d,u})_\eta^T$ are the unit displacement polarization vectors corresponding to waves with $(k_z^d)_\eta$ and $(k_z^u)_\eta$ wave vector respectively.

The displacement polarization vector $P_\eta^{d,u}$ and vertical slowness component $(m_z^{d,u})_\eta$ are determined by solving the Christoffel equation (2) and applying Snell's law $m_{//}^j = (m_x^0, m_y^0, 0)$, where j =1, 2,...N and $m_{//}^0$ is the invariant x and y projection of the slowness vector for the incident wave:

$$(C_{ijkl} m_j m_l - \rho \delta_{ik}) P_k = 0 \quad (2)$$

Where C_{ijkl} represent the layer elastic constants and ρ the density.

The stress component vector on the x-y plane $\sigma_j = (\sigma_{31}^j, \sigma_{32}^j, \sigma_{33}^j)^T$ parallel to the layer surface can be related to each of the plane wave displacement field using Hook's law:

$$\sigma_j = \sum_{\eta=1}^{3} \left(a_\eta^d d_\eta^d e^{i\omega m_z^d (z - z_{j-1})} + a_\eta^u d_\eta^u e^{i\omega m_z^u (z - z_j)} \right)_j e^{i\omega (m_x x + m_y y - t)} \quad (3)$$

Where the components $(d_i^{d,u})_j$ of vector $d_j^{d,u}$ are related to the polarization vector $(P_j^{d,u})$ by [8]:

$$(d_i^{d,u})_j = (C_{i3kl}\, m_l P_k^{d,u})_j \quad (4)$$

The displacement u_j and stresses σ_j on the upper and lower interfaces bounding layer j can be represented in matrix form

$$\begin{Bmatrix} u_j^- \\ u_j^+ \end{Bmatrix}_j = \begin{bmatrix} P_j^d & P_j^u H^u \\ P_j^d H^d & P_j^u \end{bmatrix}_j \begin{Bmatrix} A_j^d \\ A_j^u \end{Bmatrix} \quad (5.a)$$

$$\begin{Bmatrix} \sigma_j^- \\ \sigma_j^+ \end{Bmatrix}_j = \begin{bmatrix} D_j^d & D_j^u H^u \\ D_j^d H^d & D_j^u \end{bmatrix}_j \begin{Bmatrix} A_j^d \\ A_j^u \end{Bmatrix} \quad (5.b)$$

Where $P_j^{d,u}$ (3x3) matrix gathers together polarization vectors, $A_j^{d,u}$ the amplitude vectors of the waves going down (*d*) and up (*u*) and $H^{d,u}$ a diagonal matrix which contain the corresponding wave phase shift and $D_j^{d,u}(3\text{x}3) = [d_1^{d,u}, d_2^{d,u}, d_3^{d,u}]$.

By mean of matrices (3x3) several physical magnitudes as reflection and transmission energy coefficients could be easily computed. This becomes possible because stresses and displacements at the top (j = 0) and the bottom (j = N) interfaces of the multilayer are related together by application of the recursive procedure. The cell stiffness matrix K_c [8] connecting separately displacements and stresses, on the level of the two interfaces of the jth layer, is obtained by substituting into Eq. (4.a) the amplitude vector $A_j^{d,u}$ from Eq.(4.b).

$$K_c(6\text{x}6) = \begin{bmatrix} D_j^d & D_j^u H^u \\ D_j^d H^d & D_j^u \end{bmatrix}_j \begin{bmatrix} P_j^d & P_j^u H^u \\ P_j^d H^d & P_j^u \end{bmatrix}_j^{-1} \quad (6)$$

The recursive algorithm leads to the global stiffness matrix K, which relates displacements (u_0, u_N) to stresses (σ_0, σ_N), subscripts 0 and N refer to the first and the last interface. To find the Floquet wave properties one applies the periodicity conditions [8,10]

$$\begin{bmatrix} u^+ \\ \sigma^+ \end{bmatrix} = e^{i\lambda h_c} \begin{bmatrix} u^- \\ \sigma^- \end{bmatrix} \quad (7)$$

where λ is the Floquet wave number component in the z direction and h_c the thickness of the unit cell. It relates the stresses and displacements on the top (σ^-, u^-) and bottom (σ^+, u^+) surfaces of the cell (Fig.1).

2.2 Reflection-transmission coefficients

The results provided in this paper have been obtained for quasi-isotropic composite with [0/45/90/-45] cells. The composite laminate with total thickness 2.88 mm has 24 laminas (6 superlayers); the thickness of each lamina is 0.12 mm. The properties of the lamina used in the model are those determined by Potel and al [5] given in table.1: the constants are complex, in other words the medium is a lossy one.

Table1. Elastic constants in GPa for a carbon/epoxy medium from Ref.5 if the sixth-order symmetry A6 axis is parallel to the (Oz) axis.

C_{11}	13.7+0.13j
C_{12}	7.1+0.04j
C_{13}	6.7+0.04j
C_{33}	126+0.73j
C_{44}	5.8+0.1j
ρ (kgm^{-3})	1577

Basing on the stiffness matrix method and the boundary conditions, we can calculate the reflection and transmission coefficients R, T by admitting that the stresses σ_{23}^0, σ_{13}^0 and σ_{23}^N, σ_{13}^N in the multilayered one on the level of the interfaces with water are equal to zero. We can thus write displacements with these interfaces according to the stresses:

$$u_3^0 = S_{11}(3,3)\ \sigma_{33}^0 + S_{12}(3,3)\ \sigma_{33}^N \quad (8)$$

$$u_3^N = S_{21}(3,3)\ \sigma_{33}^0 + S_{22}(3,3)\ \sigma_{33}^N \quad (9)$$

With S_{ij} are blocks (3, 3) of the global compliance matrix: $S = K^{-1} = \begin{bmatrix} S_{11} & S_{12} \\ S_{21} & S_{22} \end{bmatrix}$.

By writing displacements and stresses according to the reflection and transmission coefficients and by taking account of the boundary conditions, we can calculate the reflection and the transmission coefficients (R) and (T).
The time-averaged energy density can be calculated and given by [9]

$$P_i = -\frac{1}{2}\mathrm{Re}(S_{ij}\sigma_{ij}^{*}), \qquad (10)$$

Where S_{ij} is the stress tensor and σ_{ij}^{*} the complex conjugate of the strain tensor.

2.3 Multilayered Rayleigh and Lamb and waves

The characteristic equation for Lamb modes can be determined from the total stiffness matrix of the structure K or its inverse, the global compliance matrix S. If the top and bottom surfaces are free, the Lamb wave dispersion equation is determined as [10]

$$\det(K) = 0 \qquad (11)$$

The characteristic equation for multilayered Rayleigh wave in a semi infinite layered structure is also can easily be found from the total stiffness matrix..
When the total layered system thickness or the frequency increase, the wavelength is less than the lamina thickness; the solution will approach for a semi-infinite periodic medium with properties of the top lamina. In this situation we will underline the existence of surfaces waves which were called multilayered Rayleigh waves and their correspondence with the combination of Floquet waves. The multilayered Rayleigh wave is a linear combination of three inhomogeneous Floquet waves.
In Ref [5], Potel and al give several conditions on the propagation of multilayered Rayleigh waves that must satisfies: the cancellation of a (3x3) determinant corresponding to the boundary conditions for a vacuum/infinite anisotropic periodically multilayered medium structure. Moreover, the modulus of the reflection coefficient for a non lossy medium must be equal to one, whereas that of a lossy medium present a trough. Another important property is that all the Floquet waves must be inhomogeneous.
Here, we will first confirm the conditions given by Potel et al [5]. Second, compare the numerical result for the reflection phenomena and the spectrum of pass and stop bands for three Floquet waves for [0/45/90/-45] composite. Finally, a density energy criterion on the propagation of guided waves (multilayered Rayleigh wave and Lamb wave) is given.

At oblique incidence of ultrasonic waves on a multiply composite sample immersed in the water, the reflection-transmission coefficients are calculated using Eq.(8), (9). Here we theoretically investigate wave reflection through a $[0/45/90/-45]_6$ composite.
Fig.4 (a) and Fig.4 (b) show the reflection coefficient for a multi-ply composite with 24 layers $[0°/45°/90°/-45°]_6$ layout with a total thickness 2.88 mm). The incident plane is oriented at 0° relative to the top lamina and at different frequency. The solid line corresponds without attenuation and the dashed line with attenuation.
Starting from 2.5 MHz frequency, the critical angles between 0° and 50° were detected. Once a critical angle was found, the same critical angle was sought by changing the ultrasonic frequency. Frequency step sizes were increased by increments of 0.1 MHz while the incident angle step size was 0.1°. It should be noted here that representing the critical angle as a function of the frequency is equivalent to representing the velocity of the mode as a function of the frequency. If the medium of reference is water, the multilayered Rayleigh wave or the leaky lamb wave speed is given by

$$V_R = \frac{V_{water}}{\sin\theta_R} \qquad (12)$$

where θ_R is the Rayleigh angle.

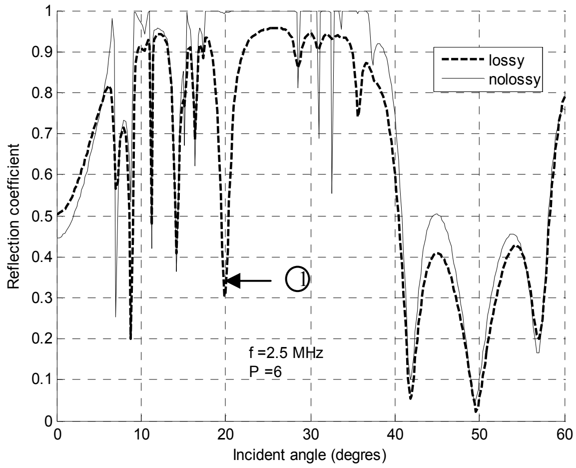

Fig.2 (a): Reflection coefficient as function of incident angle of $[0/45/90/-45]_6$ carbon-epoxy at 2.5 MHz frequency.

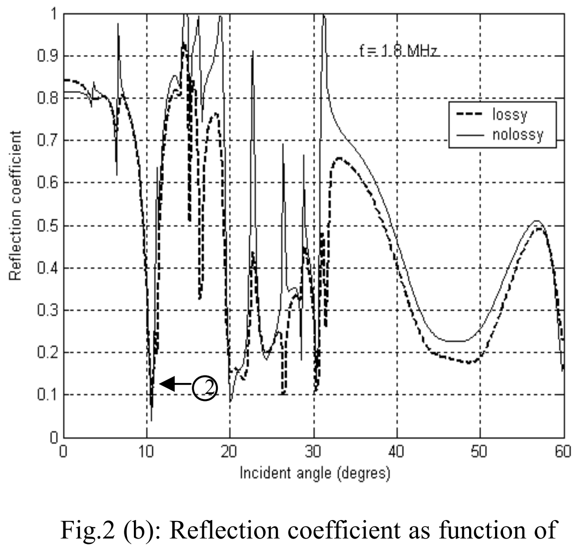

Fig.2 (b): Reflection coefficient as function of incident angle of $[0/45/90/-45]_6$ carbon-epoxy at 1.8 MHz frequency.

To analyse the mode detected numerically above, the spectrum of pass-stop bands for the three Floquet waves for [0/45/90/-45] periodic structure is represented as a function of incident angle θ and frequency with the propagation plane oriented at $\Phi = 0$ as shown in Fig.3.
White domains correspond to all three propagating waves, light gray to two propagating waves and darker gray to one propagating wave, black corresponds to the stop band for all three waves (no propagating waves permitted). In the same figure 3 is plotted the variation of critical angle with the frequency (dotted line), in other words, the dispersion curve of this mode. It can be seen that the dispersion of the mode is placed in different region of the Floquet waves pass and stop bands. This implies that the mode character change from leaky lamb wave to multilayered Rayleigh wave as will be displayed below.

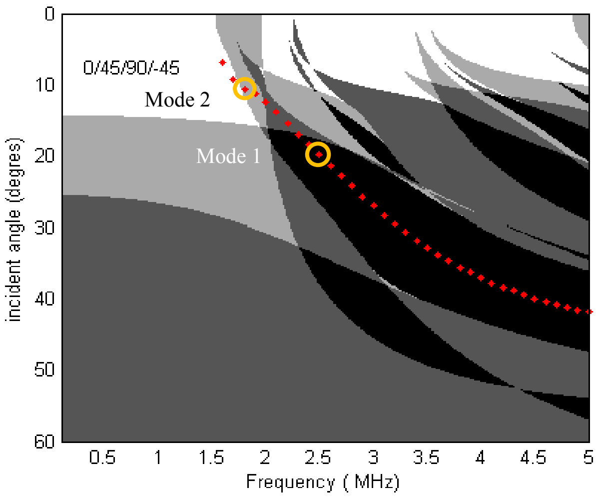

Fig.3: Spectrum of pass-stop band of [0/45/90/-45] carbon-epoxy.

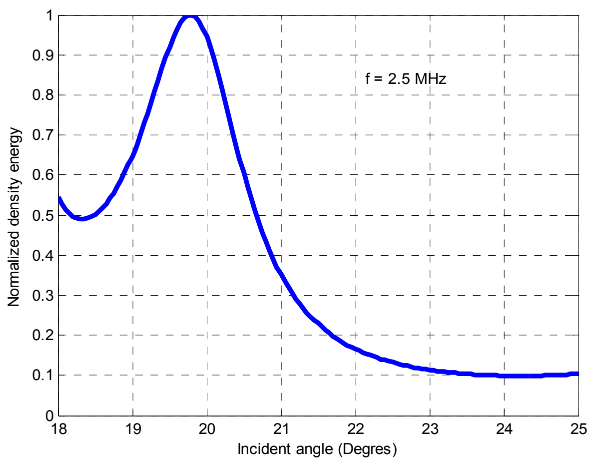

Fig.4 (a): Normalized density of energy of $[0/45/90/-45]_6$ carbon-epoxy versus incident angle at 2.5 MHz frequency.

Furthermore, the analysis of the Floquet waves stop and pass bands given in Fig.3 displays that all the Floquet waves are inhomogeneous at 2.5 MHz and the incident angle is 19.8 (This mode is located in the stop band "black zone"). This satisfies the conditions given by Pot et al [5] to obtain multilayered Rayleigh wave. The determination of the critical Rayleigh angle can also be carried out where an abrupt maximum of the normalized density of energy occurs at the critical angle. In fact, the plot of density of energy versus incident angle is given by Fig.4 (a), displays that the energy increases quickly when the incident angle changes from 18 to 25 degrees. The maximum of value is obtained at the incident angle of 19.8°.
As confirmation of these numerical results, Fig.5 and Fig.6 show the computed normal displacement profile along the thickness or depth of the plate. For the propagation of the multilayered Rayleigh waves (mode 1), it can be seen that the amplitudes of the normal displacement or normal stress are negligible at the end of the medium. The reason of this approach is that for high frequencies the material behaves increasingly like a thick slab and hence the coupling between the upper and lower boundary surfaces is reduced. However, for the propagation of lamb wave (mode 2), the normal displacement affect the entire multilayer. Let us see now, for frequencies inferior to 2.5 MHz, at frequency equal to 1.8 MHz. The critical angle dip is almost equal to 11.14° as shown in Fig. 2(b). The modulus of the reflection coefficient drops almost to zero. Fig.4 (b) shows the normalized density of energy versus the incident angle. From this figure we can observe that the density of energy increases very fast when the incident angle changes from 11 to 11.4° degrees. Its maximum position is also at incident angle of 11.14°. In addition, if we analyse the Floquet waves of stop and pass bands given in Fig.3, we can perceive, at this frequency and incident angle, only one non propagative Floquet waves exists. Consequently, the multilayered Rayleigh wave is converted to a leaky lamb wave for the plate. This indicates the propagation of multilayered Rayleigh wave.

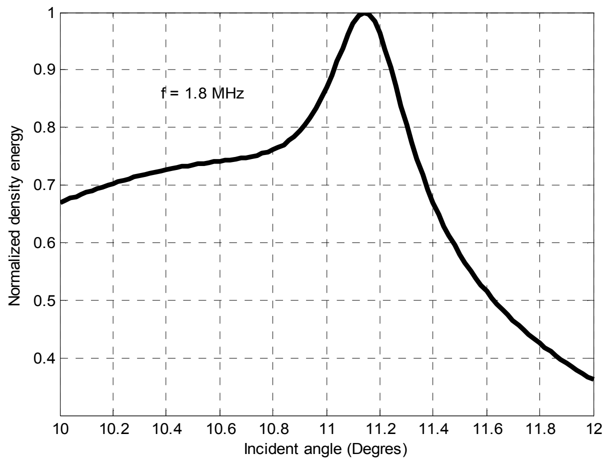

Fig.4 (b): Normalized density of energy of $[0/45/90/-45]_6$ carbon-epoxy versus incident angle at 1.8 MHz frequency.

4 Conclusion

In this paper, dispersive guided wave propagation through a loss multilayered composite immersed in water have been investigated. When the viscoelasticity of the medium is considered, the modulus of the reflection presents a trough at the Rayleigh angle whereas equal to one when lossless. Our interest is focused on a guided mode inside the frequency range 1.6-5 MHz. Within the considered frequency range, this mode has been pointed out by both reflection coefficient and density of energy analysis in term of incident angle. The propagation of guided waves is characterized by an abrupt maximum of the density of energy at the critical angle. Normal displacement field along the depth of the plate have been represented in two cases: lamb wave and multilayered Rayleigh wave. In the first case, it can clearly show how the normal displacement or stress affects all the plate. In the second case, the amplitude decays along the depth of the plate as the mode propagates through. As a result, when the frequency is increased the mode changes from a plate mode to a surface mode.

References

[1] S. I. Rokhlin and L. Wang, ''Ultrasonic waves in layered anisotropic media:Characterization of multidirectional composites,'' Int. J. Solids Struct. 39, 4133–4149 (2002)

[2] D. E. Chimenti and A. H. Nayfeh, ''Ultrasonic reflection and guided wave propagation in biaxially laminated composite plates,'' J. Acoust. Soc. Am.87, 1409–1415 (1990).

[3] Sang-Ho Rhee, Jeong-Ki Lee, Jung-Ju Lee "The group velocity variation of Lamb wave in fiber reinforced composite plate" Received 14 October 2005; received in revised form 26 June 2007; accepted 6 July 2007.

[4] C. Potel, J.F. de Belleval, E. Genay, Ph. Gatignol, "Behavior of Lamb waves and multilayered Rayleigh waves in an anisotropic periodically multilayered medium: application to the long-wave length domain" Acta Acust. 82 (5) 738–748, (1996).

[5] C. Potel, Stefaan Devolder , Aziz Ur-Rehman, Oswald Leroy & Martine Wevers "Experimental verification of the theory of multilayered Rayleigh waves" J. Appl. Phys., Vol. 86, No. 2, 15 July (1999).

[6] J. D. Achenbach, C. T. Sun, and G. Herrmann, J. Appl. Mech. 35, 689– 696 (1968).

[7] P. J. Shull, D. E. Chimeti, and S. K. Datta, J. Acoust. Soc. Am. 95, 99–105 (1994)

[8] S. I. Rokhlin and L. Wang "Stable recursive algorithm for elastic wave propagation in layered anisotropic media: Stiffness matrix method" J. Acoust. Soc. Am. 112(3), 822–834 (2002)

[9] B. A. Auld, Acoustic Fields and Waves in Solids. vol. 1, New-York: Wiley (1973).

[10] L.Wang, S.I.Rokhlin, "Floquet wave homogenization of periodic anisotropic media" J. Acoust. Soc. Am., Vol. 112, No. 1, p .38-45 (2002)

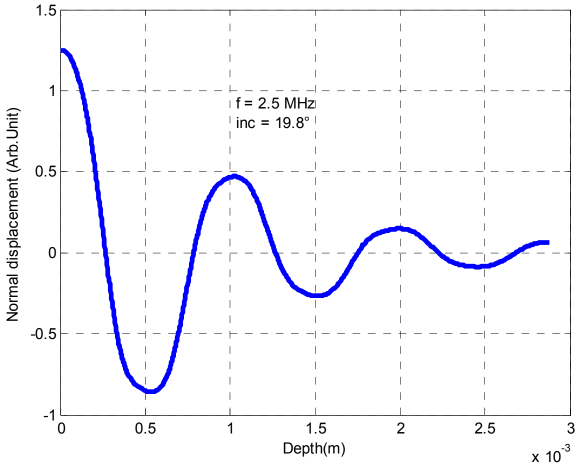

Fig.5 (a): Normal displacement (U_3) of $[0/45/90/-45]_6$ carbon-epoxy versus depth at 2.5 MHz frequency and 19.8° (multilayered Rayleigh mode).

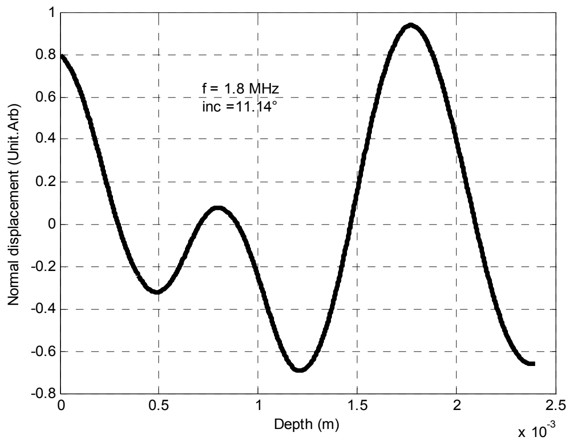

Fig.6 (a): Normal displacement (U_3) of $[0/45/90/-45]_6$ carbon-epoxy versus depth at 1.8 MHz frequency and 11.14° (lamb mode).